引用格式：CUI Ying，HE Jun-hua，WU Bing-jing，*et al*. Design of X-ray Microscope Employing Toroid Mirrors Working at Grazing-incidence[J]. *Acta Photonica Sinica*，2019，**48**(12)：1211002
崔莹，何俊华，吴冰静，等.掠入射式超环面反射镜组 X 射线显微镜设计[J].光子学报，2019，**48**(12)：1211002

掠入射式超环面反射镜组 X 射线显微镜设计

崔莹[1,2,3]，何俊华[1]，吴冰静[1]，闫亚东[1]，许瑞华[1]
（1 中国科学院西安光学精密机械研究所，西安 710119）
（2 中国科学院大学，北京 100049）
（3 武警工程大学 装备管理与保障学院，西安 710086）

摘　要：为了实现对激光惯性约束聚变中物理过程的诊断，建立了 X 射线显微成像系统.对该系统所采用的超环面镜成像特性、系统的光学设计、像差分析、公差分析和装调方法进行了研究.首先，以等离子体诊断的要求为依据确定了部分光学系统参数，设计了由 U 型排布的两个超环面镜和一个用于谱选择的平面镜构成的显微成像系统.根据消像散聚焦初步确定三个反射镜的结构参数，并利用光学设计软件进行了优化.接着，分析了 X 射线显微镜的球差、彗差、视场倾斜和像散.通过分析系统参数变化对成像质量的影响，根据系统精度要求确定了合理的公差.最后，针对离线超环面镜离轴掠入射装调问题，设计了一种辅助光学系统，并为在线高精度系统装调设计了一种双向双目交汇瞄准系统.实验结果表明：显微成像系统在物方视场 500 μm 处的分辨率优于 5 μm，基本满足激光等离子体 X 射线成像的大视场和高分辨等要求.

关键词：光学系统设计；显微成像；掠入射；超环面；X 射线
中图分类号：O439；TH74　　**文献标识码**：A　　**doi**：10.3788/gzxb20194812.1211002

Design of X-ray Microscope Employing Toroid Mirrors Working at Grazing-incidence

CUI Ying[1,2,3], HE Jun-hua[1], WU Bing-jing[1], YAN Ya-dong[1], XU Rui-hua[1]
(1 *Xi'an Institute of Optics and Precision Mechanics, Chinese Academy of Sciences, Xi'an*, 710119, *China*)
(2 *University of Chinese Academy of Sciences, Beijing*, 100049, *China*)
(3 *College of Equipment Management and Support, Engineering University of PAP, Shaanxi, Xi'an*, 710086, *China*)

Abstract: In order to diagnose the physical process of laser inertial confinement fusion, a X-ray microscope was established. The imaging characteristics of the toroidal mirrors used in the system, optical design and parameter optimization, aberrations and tolerance analysis of the system and alignment were studied. Firstly, based on the requirements of plasma diagnosis, some optical system parameters were determined, and the the microscope for imaging the X-ray through the basic structure of two tandem toroidal mirrors in u-shaped arrangement and one planar mirror for spectrum selection was designed. The structural parameters of the three mirrors were preliminarily determined according to the anastigmatic focusing. Then the optical design software was used for modeling and optimization. The spherical aberration, coma aberration, field obliquity and astigmatism of X-ray microscope were also

Foundation item: The National Key Research and Development Program of China (No.2017YFA0403300)
First author: CUI Ying (1981－), female, lecturer, Ph.D. degree candidate, mainly focuses on X-ray imaging, optical design. Email: cuiying@opt.cn
Corresponding author: HE Jun-hua (1968－), male, professor, M.S. degree, mainly focuses on digital optical information processing and digital holography. Email: hejunhua@opt.ac.cn
Received: May 27, 2019; **Accepted**: Jul.27, 2019

analyzed. By analyzing the influence of system parameters change on the image quality and the accuracy requirement of the system, reasonable tolerance was established. Finally, An auxiliary aiming system was designed to solve the off-axis problem of grazing incidence mounting of the toroid mirrors when adjusted offline, also a bidirectional binocular intersection online aiming system was designed to solve the problem of assembling and aiming accuracy of the system. Experiment results show that the resolution of the microscope is less than 5 μm at 500 μm field of view, which basically meets the requirements of large field of view and high resolution in laser plasma hard X-ray imaging.

Key words: Optical design; Microscope; Grazing incidence; Torus; X rays

OCIS Codes: 110.0180; 110.2960; 110.7440; 080.2740; 080.4225

0 Introduction

In order to achieve Inertial Confinement Fusion (ICF), high-power laser beams or particle beams are used to irradiate fusion fuels, which are compressed to high temperatures (above 5 000℃) with high density (600 g/cm^3). X-ray microscopy which image the X-rays emanating from a laser-produced plasma provides an effective way to diagnose the spatial characteristics of laser plasma, which plays an important role in the study of laser radiation uniformity[1], implosion compression symmetry[2] and fluid instability[3-4]. Since the refractive index of any materials to X-ray is lower than 1, and X-ray is strongly absorbed by materials, refraction imaging commonly used in the visible light band can not be used. When a glancing angle to a surface is small, the X-ray is totally reflected by the surface, the grazing incidence system is generally used according to the full external reflection. The structural forms of the grazing incidence reflection X-ray microscope system used for ICF experimental research predominantly come in two sorts: One is the Kirkpatrick-Baze (KB) structure firstly created by Kirkpatrick and Baze in 1948(two orthogonal cylindrical or spherical grazing-incidence mirrors reflecting the X-ray), AKB and KBA structure based on KB structure (two parallel spherical mirrors are applied to the meridian and sagittal surfaces)[5-7]. The other one is the rotational axisymmetric grazing-incidence reflection system developed by Wolter in 1952 (confocal combination of spheroid and hyperboloid is used to realize the ideal imaging that decreasing the spherical aberration and coma)[8].

The on-axis aberration of a grazing-incidence spheric-based Kirkpatrick-Baez compound microscope may be precisely corrected. However, for finite fields, the off-axis performance degrades too rapidly for high-spatial-resolution imaging of even the smallest objects of interest[9-10]. The Wolter configuration is a coaxial confocal optical system, which can be used as one of the high resolution imaging to eliminate spherical aberration of the point on the axial and it can effectively reduce off-axial aberration such as coma aberration. However, due to its closed annular design, for high energy X-ray imaging, it is difficult to achieve the required smoothness and surface tolerance [11-12], which will cause serious X-ray scattering, resulting in the decline of resolution. In order to get high resolution in larger field of view in X-ray region, providing basis for ICF diagnosis, the system adopts two toroid mirrors which are nearly parallel to image the target for the compactness requirements of the structure of imaging system, and the image aberration can be decreased to acceptable level. An auxiliary aiming system and the bidirectional binocular intersection online aiming system ensure the precision of the mirrors' alignment.

1 Design of the microscope

The principle of this imaging system combines the characteristics of the KB mirrors and the Wolter microscope. In order to be compact and correct aberrations, toroid mirrors are used instead of two orthogonal cylindrical mirrors in the system. The toroid shapes also present some advantages of brightness compared to KB cylindrical mirrors because only a single toroid mirror can be used to achieve two-dimensional focusing imaging. Toroid surfaces have the same imaging qualities as quadric surfaces (i.e. elliptical and parabolic) and are easier to polish.

1.1 Toroid mirror and focusing characteristic

As shown in Fig.1, A toroid is a surface of revolution generated by revolving a circle, whose radius is r, about the axis Z which is coplanar with the circle and a distance R from the center of the circle.

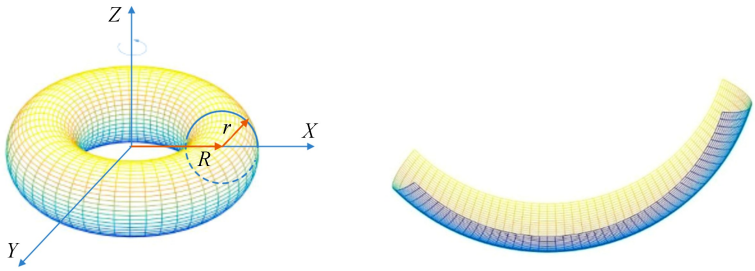

Fig.1 Schematic diagram of toroid mirror

The toroid surface equation in Cartesian coordinates can be written as [13]

$$f(x,y,z)=\left(\sqrt{x^2+y^2}-R\right)^2+z^2-r^2 \tag{1}$$

where R is the major radius, and r is the minor radius. Toroid mirror is a part of the concave surface, and the base arc can be defined as

$$S=\frac{rx^2}{1+\left[1-(1+k_x)r^2x^2\right]^{1/2}}+\sum_{i=1}^{p}A_i x^{2(i+1)} \tag{2}$$

where k_x is the conic constant, and A_i is polynomial aspheric coefficients. Usually the meridian radius of curvature R is typically quite large (10^5 mm for our mirror) in comparison with sagittal radius of curvature r, so a toroid mirror becomes a feasible approximation to the ideal ellipsoidal figure. Its advantage is that a single mirror can be used to achieve two-dimensional focusing imaging instead of KB structure. It is of a simple structure and can constitute a multi-channel system. In addition, toroid mirrors could be more easily polished than quadratic surfaces.

It can be seen that the toroid mirror also has an axis of rotational symmetry, but it does not coincide with the axis of the optical system. Toroid mirror is a feasible approximation to the ideal ellipsoidal mirror when the meridian radius of curvature R is typically quite large in comparison with all the other dimensions of the microscope. Because the toroid mirror has different radius of curvature in meridian plane and sagittal plane, it can be considered separately when focusing. The focused imaging on the meridian plane is essentially the same as the imaging characteristics of a spherical mirror, which has been analyzed in many literatures[14-15].

The best way to focus the beam with a single element is the use of a toroid mirror with unity magnification (Rowland configuration), which cancels the astigmatism and the coma. However, when a big magnification is required, coma aberration is unavoidable. Therefore, two toroid mirrors are used to improve the coma caused by the single toroid mirror which does not satisfy the Abbe sinusoidal condition, so as to improve the imaging quality of the off-axis point.

1.2 Initial parameters of optical structure

As an imaging optical system, the aim of the proposed configuration is to provide a high resolution image of the X-ray source with the following primary concerns.

The focal length and diameter of the mirrors determine not only the size of the system, but also the resolution of the optical system. Because the energy ICF is high, the environment surrounding the micro ball of Deuterium (D) and Tritium (T) nuclei is more complex. It's better to place the imaging system in a place far from the target, avoiding the damage of high energy beams and debris. Therefore, the object distance of the microscope is better more than 500 mm. At the same time, considering the limitation of the space for installing the microscope, assuming the magnification 15×.

When design the grazing incidence optics, the glancing angle must firstly be decided at the center points of the mirrors.The critical angle of reflection depends on the surface material and wave length of the X-ray. As the wavelength of X-rays becomes shorter and shorter, the critical angle of reflection is extremely small. However the mirrors should have sufficient reflectivity at a large grazing angle. And the design of the grazing angle should take into account the float of the incident angle because of the off-center edge of the mirrors. The grazing incident angle is set to $\theta=0.5°$, achieved by using the multilayer.

The field of view of the microscope is determined by the size of the implosion compression region, which is only several microns, the ideal Field of View (FOV) restricted to 1 mm will be sufficient.

The structure of X-ray microscope is shown in Fig. 2. The system consists of three mirrors, two of

them are toroid mirrors with the same radius of curvature, and the third one is a plane mirror. The first two mirrors M1 and M2 are arranged in a u-shape with an angle to converge the X-rays both on the meridian plane and sagittal plane.

Since the third mirror is plane who only deflects the optical axis and does not focus the light, only the first two toroid mirrors are considered in the calculation of the initial structural parameters. As shown in Fig. 3, AO_1O_2A' is the pseudo-axis of the optical system. The gracing incident angle of the first mirror M1 is $\theta_1=0.5°$ and the incident angle of the second mirror M2 is $\theta_2=0.5°$, according to the geometrical relation of reflection imaging, a formula about angles can be obtained as follows

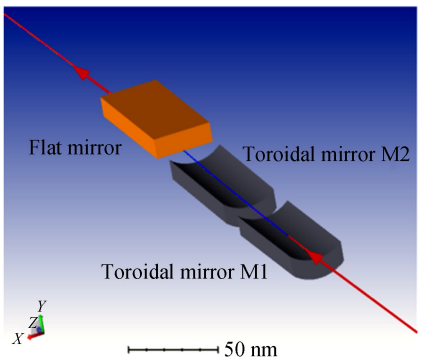

Fig.2 Schematic diagram of X-ray imaging system

$$\angle A+\angle A'=4\times0.5°=2° \tag{3}$$

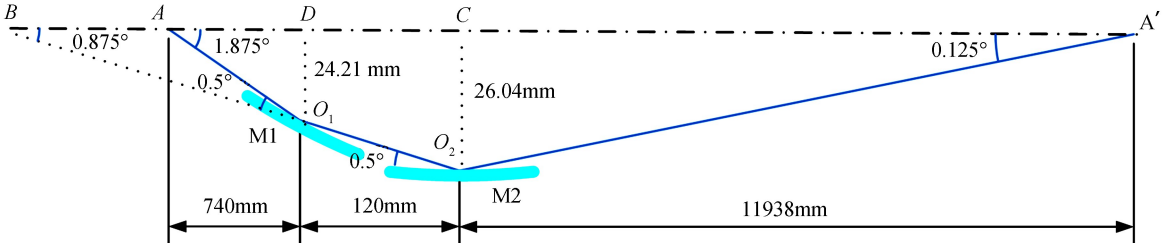

Fig.3 Reflective imaging diagram of double toroid mirrors

And the magnification can be approximately defined as $M=\angle A/\angle A'=15$, combined with the Eq. (3), we got $\angle A=1.875°$, $\angle A'=0.125°$. Assuming that the distance from the object A to the center of the first toroid mirror O_1 is $p_1=AO_1=740$ mm, and the distance between the two mirrors is $d=O_1O_2=120$ mm, then according to the triangle cosine relation, it can be calculated that the distance from the center of the second mirror O_2 to the image A' is $q_2=A'O_2=11\ 938$ mm. The object distance p_2 of the second mirror and the image distance q_1 of the first mirror satisfy the following equation

$$p_2=q_1-d \tag{4}$$

The total magnification M of the microscope and two toroid mirrors' respective magnification M_1 and M_2 meet the following requirements

$$M=M_1M_2=\frac{q_1}{p_1}\frac{q_2}{p_2}=\frac{q_1}{740}\frac{11938}{q_1-d}=15 \tag{5}$$

Then the following quantity can be figured out: $q_1=-1\ 589$ mm, $M_1=2.14$, $M_2=6.985$.

In the case of grazing incidence, the optical axis of the thin beam does not coincide with the normal line of the mirror on the incident point, and the light is no longer a concentric beam after reflection by the optical system, which is focused in the meridian and sagittal direction respectively, and its relationship satisfies the Young's formula

$$\frac{n'\cos^2 i'}{q_m}-\frac{n\cos^2 i}{p_m}=\frac{n'\cos i'-n\cos i}{R} \tag{6}$$

$$\frac{n'}{q_s}-\frac{n}{p_s}=\frac{n'\cos i'-n\cos i}{r} \tag{7}$$

where p_m and q_m are the object distance and image distance in the meridian plane respectively; p_s and q_s are in the sagittal plane; i is the incident angle and i' is the exit angle; n and n' are the refractive index of object space and image space. R is the radius of meridian curvature of the toroid mirror and r is the radius of sagittal curvature. Then the grazing incident angle $\theta=\pi/2-i$, $i'=i$, $n'=-n$, $p_m=p_s=p$. According to Eq. (8) and Eq. (9), the meridian focal length f_m and sagittal focal length f_s of a toroid mirror can be obtained.

$$\frac{1}{f_s}=\frac{1}{p}+\frac{1}{q_s}=\frac{2\sin\theta}{r} \tag{8}$$

$$\frac{1}{f_m}=\frac{1}{p}+\frac{1}{q_m}=\frac{2}{R\sin\theta} \tag{9}$$

During the optical design of the microscope, associated with the initial structural parameters (p, M, θ, d), a unique set of toroid mirrors' parameters could be established. In order to make the object be imaged on the same position both on meridian plane and sagittal plane, the focus of both direction should be equal:

$$f_{1m}=f_{1s}=f_1=1\ 385\ \text{mm} \tag{10}$$

which is substituted into Eq.(8) and Eq.(9), then we get the meridian radius of the first mirror R_1 and sagittal radius r_1 respectively.

$$R_1=\frac{2f_{1t}}{\sin\theta}=\frac{2\times 1\ 385\ \text{mm}}{\sin 0.5^\circ}=317\ 422\ \text{mm} \tag{11}$$

$$r_1=2f_{1s}\sin\theta=2\times 1\ 385\ \text{mm}\times\sin 0.5^\circ=24.17\ \text{mm} \tag{12}$$

In the same way, we get the radius of the meridian plan R_2 and radius of sagittal plane r_2 of the second mirror.

$$f_{2t}=f_{2s}=f_2=1\ 495\ \text{mm} \tag{13}$$

$$R_2=\frac{2f_{2t}}{\sin\theta}=\frac{2\times 1\ 495\ \text{mm}}{\sin 0.5^\circ}=342\ 633\ \text{mm} \tag{14}$$

$$r_2=2f_{2s}\sin\theta=2\times 1\ 495\ \text{mm}\times\sin 0.5^\circ=26.09\ \text{mm} \tag{15}$$

This is not the only solution for the microscope structure. A set of toroid mirrors with appropriate radius of curvature can be calculated with different grazing angles, object distances, magnification and spacing of mirrors.

1.3 Optimization

The optical system can be optimized after the determination of the initial structure. Since the optical system of the grazing incidence structure is not coaxial, and the chief optical axis rotates at the break point during modeling, the grazing incidence reflection belongs to the large off-axis of the optical element, and the toroid mirror belongs to aspherical mirror, so the default evaluation function and constraint conditions cannot be used for the optimization by ZEMAX.

The mirror length l_1 of the first toroid mirror is an adjustable quantity whose length is determined by the expected spatial resolution and the geometric light gathering angle. To some extent, increasing l_1 can improve the light collection efficiency of the system, but it will damage the off-axis image quality. The second toroid mirror length l_2 can be adapted according to the first mirror length l_1, so that all (or part) of the incident light is received and reflected. A proper shortening of l_2 can act as an aperture and further improve off-axis aberration.

The radius of meridian curvature, radius of sagittal curvature of the two toroid mirrors, the distance between toroid mirrors, and object distance, image distance are all variables. The optimal evaluation function measures the imaging quality of the system by minimizing the spot radius of the image plane. The on-axis performance is modestly degraded and uniformly aberrations distributed over a chosen object field. The Spot diagram of the optimized system is shown in Fig.4.

Obviously, the spot size is sufficiently bigger than the Rayleigh limit and the microscope belongs to the large aberration system. Spot diagram is still a feasible method to evaluate the imaging quality of large aberration system, which can show the concentration and dispersion degree of point source on the image plane. According to the design parameters, ZEMAX is used to simulate the performance of the microscope, and the spot diagrams of different field of view are calculated. As shown in Fig. 4, the maximum RMS diameter of the spot in each field of view is 52 μm, which meets the requirements of system resolution in the image field of view. The results show that as the field of the object is increased, the spot on the image surface is gradually increasing.

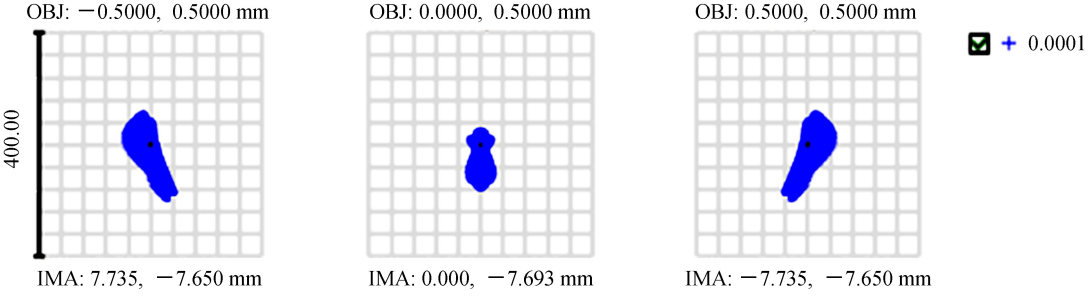

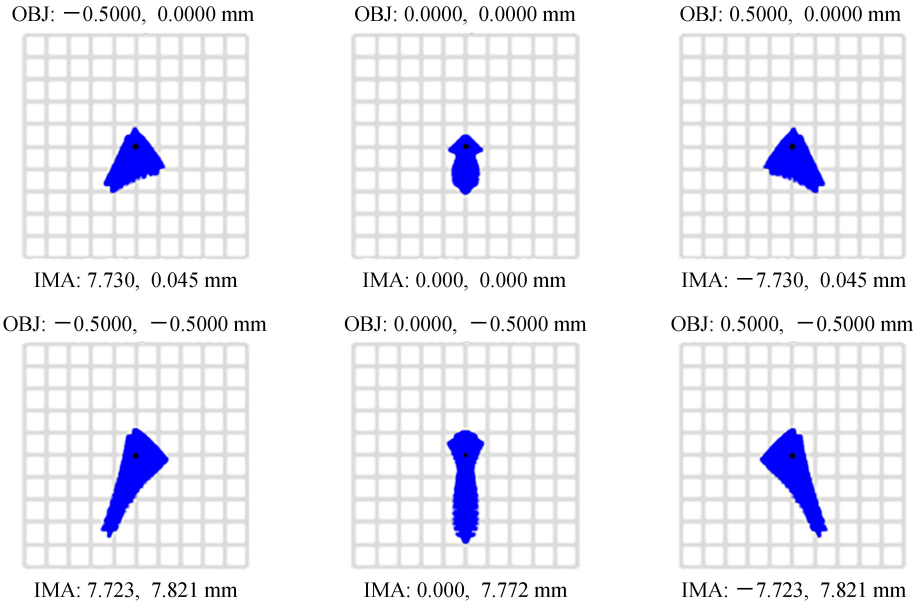

Fig.4 Spot diagram on image plane

2 Analysis

2.1 Aberrations

The biggest advantage of the reflective imaging system is with no chromatic aberration. Compared with axisymmetric optical systems (without considering high order aberrations), The aberrations cannot be analyzed by the software ZEMAX exactly, the primary aberration of off-axis reflection optical system is still spherical aberration, coma astigmatism, etc. However, coma includes linear coma and constant coma, while astigmatism contains quadratic, linear and constant terms. The pseudo axis is regarded as the optical axis, actually, incident rays are all off axis.

2.1.1 *Spherical aberration*

For a single toroid mirror, since the radius of meridian curvature is much larger than the radius of sagittal curvature, the spherical aberration is mainly sensitive to the meridian surface. The aperture longitudinal aberration is

$$\Delta_{\text{sperical}} = -\frac{3\alpha q^2(\theta R - q)}{\theta^3 R^2} \tag{16}$$

where α is the aberrant angle of the reflection ray to the center of the mirror.

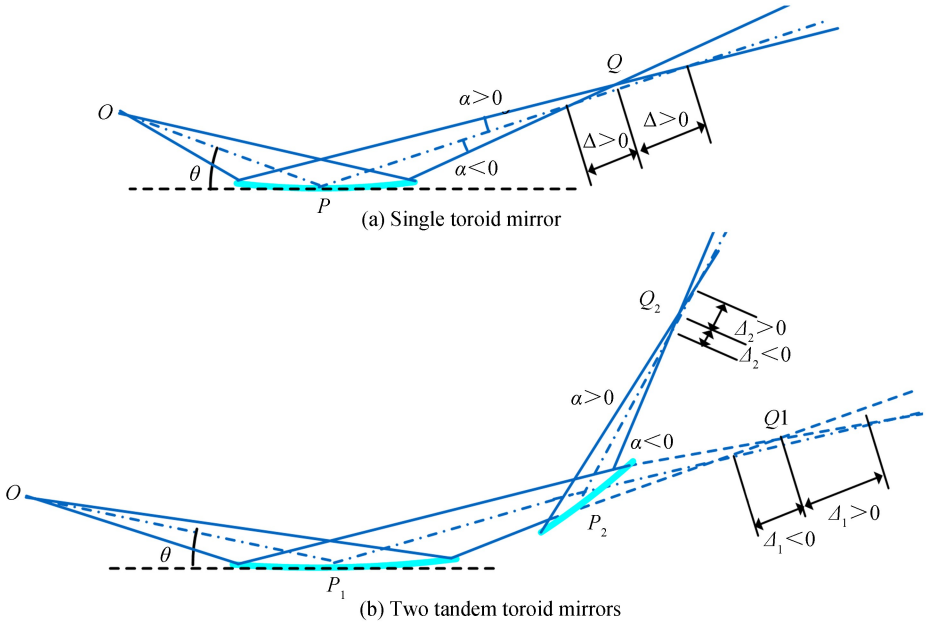

Fig.5 Longitudinal spherical aberration of single or two toroid mirrors

As shown in Fig. 5, for two toroid mirrors, with the correct choice of parameters, the spherical aberration can be corrected when

$$\Delta_1(\alpha)+\Delta_2(-\alpha)=0 \tag{17}$$

with the grazing incidence angle same and mirrors 1 and 2 facing.

2.1.2 *Coma aberration*

Due to the different magnification M of each point on the image plane, off-axis focusing is degraded, especially when the object deviates from its principal axis, and when the grazing incidence angle is small. The coma influence cannot be ignored. For a toroid mirror, the change of the scaling ratio of the beam across the length of the mirror is

$$\Delta_{\text{coma}}=(M+1)\frac{l}{4p} \tag{18}$$

As can be seen from the coma aberration formulas above, the aberrations of the toroid mirror focusing image depends on the length l of the mirror illuminated by the beam, the grazing incidence angle θ, the distance p from the mirror to the source, and the magnification M. The coma aberration can be reduced with small mirror size or large object distance.

The first mirror introduces coma, which is completely compensated by the second one, so the coma is mutually compensated with two successive mirrors configuration.

2.1.3 *Field obliquity*

As shown in Fig.6, the angle between the two mirrors is η, then the angle between the incident light and the reflective light is 2η, and the angle between them is unchanged regardless of how the incident angle changes. This is the intrinsic characteristic of the double mirror system. So, two toroid mirrors can correct the field obliquity because it satisfy the Abbe sine condition.

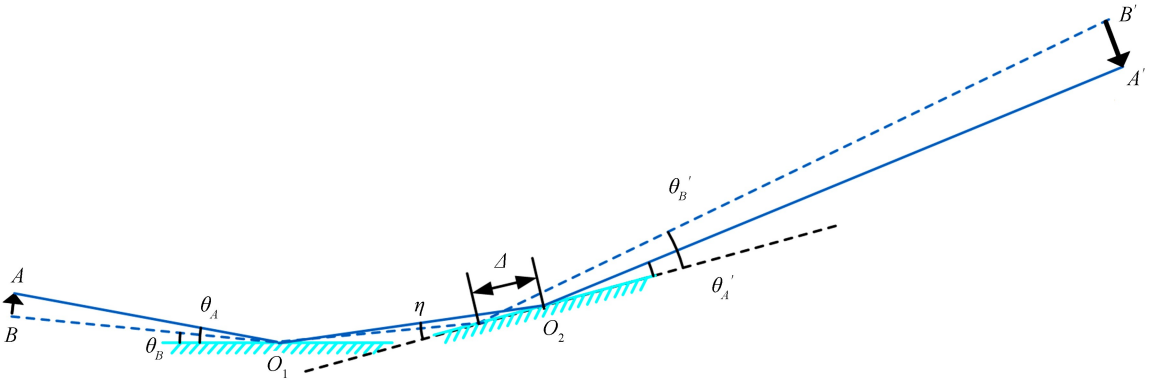

Fig.6 The character of the two toroid mirrors

2.1.4 *Astigmatism*

The only condition for overcoming astigmatism in the use of a single toroid mirror is $r/R=\sin^2\theta$, which is completely satisfied for the point on the axis, but with the increase of the field of view, the off-axis point will cause the change of the grazing incident angle, so that the sagittal and meridian image distances are not equal, and the astigmatism will appear again.

The optical structure is non-axial symmetrical, so off-axis aberration exists. When off-axis aberration has the same order of magnitude as spherical aberration, only correcting spherical aberration of points on the axis cannot guarantee the best performance of the system in the whole field of view.

2.2 Errors analysis and tolerance

In the actual assembly process, there will be errors in the parameters of each mirrors and their positions in the system, which will reduce the imaging quality of the system. Therefore, machining and assembly tolerances should be determined by the allowable quality reduction limit.

To determine the effect of each misalignment on the image quality, spot diagram in the image plane were calculated for various misalignment conditions. There are mainly four misalignment parameters: the grazing incident angle, the angle between the two toroid mirrors, the distance between the toroid mirrors, the distance from the object to the first toroid mirror.

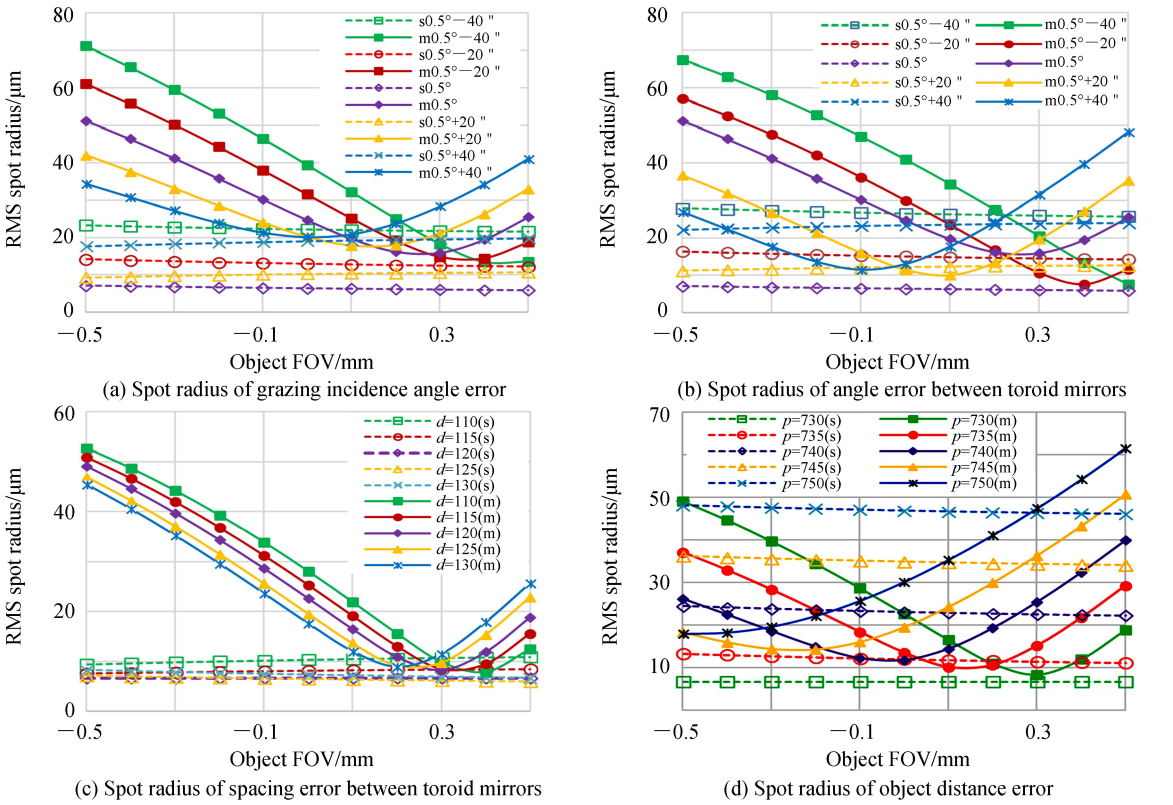

(a) Spot radius of grazing incidence angle error

(b) Spot radius of angle error between toroid mirrors

(c) Spot radius of spacing error between toroid mirrors

(d) Spot radius of object distance error

Fig.7 The influence of parameters on the performance of microscope

It can be seen from the Fig.7 that the optimal resolution position is not at the center where the chief ray intersects the image plane, but is about 0.2 mm offset to the center of the image in the positive direction of the field of view. Such imaging characteristics are related to the asymmetric structure caused by grazing incidence. Spatial resolution is more sensitive to the change of the grazing angle, and the larger the grazing angle is, the higher the imaging quality will be.

Besides the parameters analyzed above, other parameters change independently, and we evaluate the range of each tolerance, the central field resolution should be less than 2 μm under the tolerance. Then, we adjusted the tolerance so that 80% of the microscope resolution remained below 5 μm in the whole field. This calculation was obtained by randomly selecting the optical location of 60 000 previously calculated tolerances of different configurations. The final tolerances for positioning are summarized in Table 1.

Table 1 Positioning tolerances of each mirrors

	M1	M2	M3
Translation along the *X*-axis	200 μm	200 μm	500 μm
Translation along the *Y*-axis	50 μm	50 μm	50 μm
Translation along the *Z*-axis	200 μm	200 μm	1 000 μm
Rotation around the *X*-axis	0.01°	0.01°	0.01°
Rotation around the *Y*-axis	0.01°	0.01°	0.01°
Rotation around the *Z*-axis	0.1°	0.1°	0.1°

The image resolution is highly sensitive to the mirror figure. Slope errors is the error between the rugged reflecting surface and the ideal smooth surface. The coating material of the mirror is Pt, and the RMS surface roughness of the mirrors was assumed to be 0.5 nm.

3 Alignment

The microscopy system is a grazing incident imaging system which is non-axisymmetric. The accuracy of grazing angle is of great influence on imaging quality. It is difficult to achieve high accuracy by the common method used in the rotational axisymmetric structure under the condition of limited space.

3.1 Off-line mirrors mounted

Since the mirrors of microscope (including M1～M3) is to be installed in the chamber of laser fusion, the space of the chamber is quite limited, and the system requires a highly small grazing incident angle, so the installation and adjustment of the mirrors are typical difficult. Off-line adjustment is mainly to precisely align three mirrors. The fine alignment of the optical system was carried out by especially adjusting the glancing angle to mirror M1 and M2 respectively.

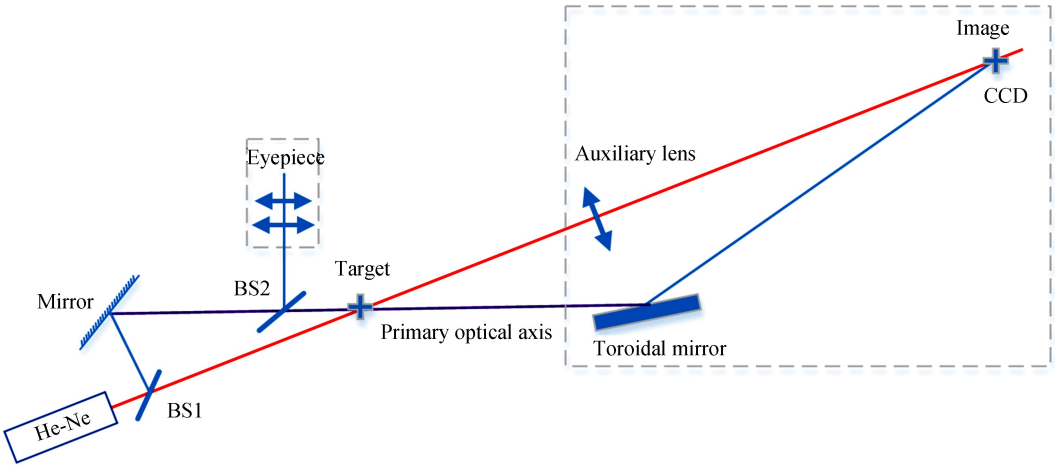

Fig.8 Auxiliary adjustment system

As shown in Fig.8, The adjustment of the toroid mirror resort to an auxiliary laser imaging, an optical lens with a large numerical aperture is adopted to be equivalent to the conjugate relationship between the object and image of the toroid mirror, the error and depth of field of the equivalent lens are designed considering the positioning accuracy requirements of the X-ray microscope. The optical structure of the auxiliary adjustment system is shown in Fig 8. BS1 and BS2 are the beam splitters. The He-Ne laser irradiates the target and forms a cross-wire image at the image plane through the auxiliary lens. The BS1 and a mirror deflects another beam of light to the main optical axis, so that the target is focused through the toroid mirror. Then the angle of the toroid mirror is adjusted, when the two images formed by the two paths of light coincide, the grazing angle is adjusted. The relative positions of the mirrors are adjusted by the manipulator which can be used to adjust all the degrees of freedom of the mirrors according to the alignment tolerances.

3.2 On-line optical alignment

Off-line mounting ensures that the internal optical elements of the microscope be installed in place, and then online alignment is required to realize that the microscope aim at the center of the object. The microscopic system is different from ordinary optical instruments in that its object and image are not in the same horizontal plane. In addition, the microscopy is installed in the chamber of laser fusion whose space is limited, causing a lot of difficulties in setting and adjusting. The binocular intersection aiming lasers is designed to realize the optical system aiming through the spatial intersection of two laser beams. For the space of the target chamber is limited, the opening angle of the two laser beams can not be too large.

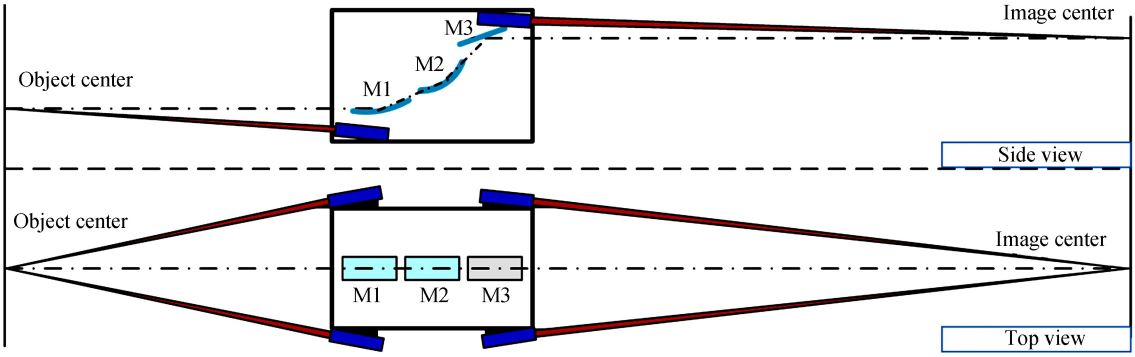

Fig.9 Schematic diagram of microscope aiming section

The aiming structure of object and image planeis shown in Fig.9. There are two pairs of tiny telephoto lenses. The lens image the target on the CCD, the microscope can be adjusted by judging the direction needs to move through the quadrant position of the center cross on the image plane. The object field of view is 6 mm×6 mm.

Image quality evaluation of binocular vision aiming system is shown in Fig.8. Figure 11 (a) is the spot diagram of the system image plane. The size of the spot is similar to the diffraction airy spot diameter, so the resolution of the object plane is 20 μm. Figure 11 (b) is the Modulation Transfer Function (MTF), The MTF values at 50 lp/mm are more than 0.3 in object field of view, which satisfies the imaging requirements.

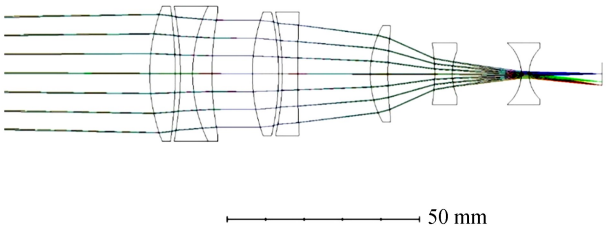

Fig.10 Optical structure of binocular vision aiming system

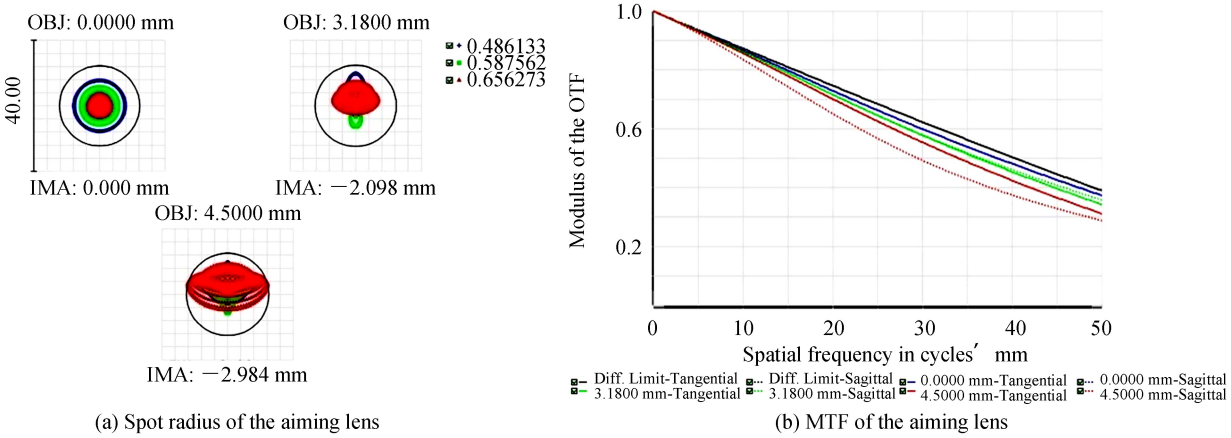

Fig.11 Image quality evaluation of binocular vision aiming system

4 Experiment and result

The source is an X-ray tube open Mo target with metal materials as the anode and filament as the cathode, and its maximum voltage is 50 kV and current is 1 mA. The imaging detector is a PI1 300×1 340 X-ray CCD camera with pixel size of 20 μm. Figure 12(a) is an image of a Ni grid, whose line width is 6 μm and the period is 20 μm. Figure 12(b) describes the light intensity distribution along the horizontal direction, the abscissa is the field of view in the object space and the ordinate is the normalized light intensity. The effective field of view can reached about 500 μm. The intensity distribution curve is essentially to image the mesh edge with Edge Response Function (ERF) in different field of view, so the (20% ~ 80%) peak-valley value of the ERF is correspond to the resolution of the image plane, which can be used to calculate the resolution of the object plane according to the magnification M, the pixels can be converted into microns which is defined as the resolution of the microscope. As shown in Fig12(c), the spatial resolution in the center of the object plane is up to 2 μm, better than 5 μm in the 500 μm field of view. The best resolution achieved and the obtained field of view was worse than the simulation results. We consider the most dominant factor is the limitation of toroid surface processing accuracy and the influence of grazing angle scattering.

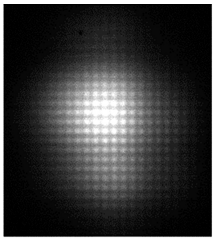

(a) Backlight image of a Ni mesh grid

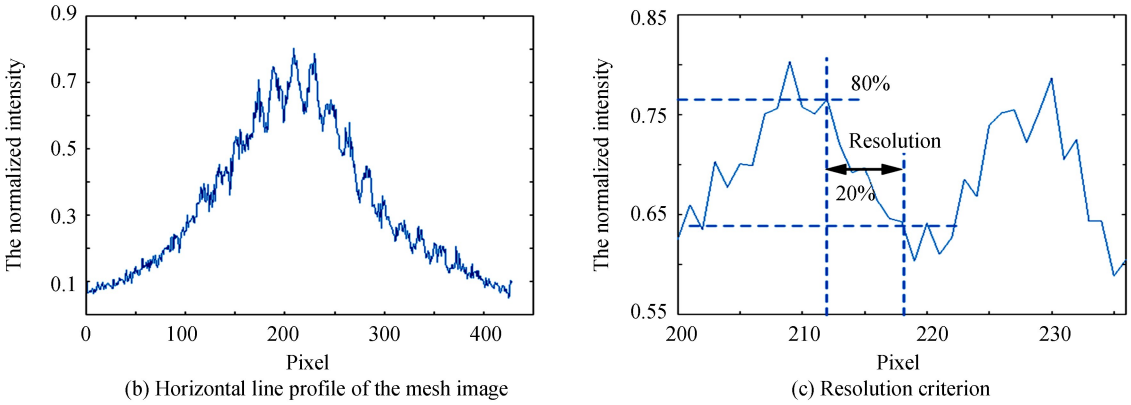

Fig.12 Backlight image of a Ni mesh grid and resolution of the image

5 Conclusion

According to the spatial resolution requirements of ICF optical diagnosis and the limitation of experimental space, the X-ray microscope based on the toroid mirrors is designed and optimized. The imaging simulation shows that the spatial resolution of the optimized system is less than 5 μm in the range of 1 mm field of view. Backlight experiments show that the resolution of the system is about 5 μm at 500 μm. The errors between experimental results and simulation results are mainly due to the influence of mirror shape accuracy and diffraction effect. The microscope basically meets the requirements of large field of view and high resolution in laser plasma X-ray imaging. The following work direction is multi-light path structure design to gather more information at the same time, and the design of the multilayer, for the increase of the grazing incidence angle would be useful for image-forming in the hard X-ray region.

References

[1] DEWALD E L, HARTEMANN F, MICHEL P, *et al*. Generation and beaming of early hot electrons onto the capsule in laser-driven ignition hohlraums[J]. *Physical Review Letters*, 2016, **116**:075003.

[2] KAGAN G, LANDAN O L, SVYATSKIY D, *et al*. Inference of the electron temperature in inertial confinement fusion implosions from the hard X-ray spectral continuum[J]. *Contributions to Plasma Physics*, 2019, **59**(2): 181-188.

[3] CAILLAUD T, ALOZY E, BRIAT M, *et al*. Recent advance in target diagnostics on the Laser Méga Joule (LMJ)[C]. SPIE, 2016: 996606.

[4] JIANG Shao-en, WANG Feng, DING Yong-kun, *et al*. Experimental progress of inertial confinement fusion based at the ShenGuang-III laser facility in China[J]. *Nuclear Fusion*, 2018, **59**(3): 102308.

[5] MATSUYAMA S, EMI Y, KINO H, *et al*. Achromatic and high-resolution full-field X-ray microscopy based on total-reflection mirrors[J]. *Optics Express*, 2015, **23**(8): 9746-9752.

[6] ZHAO Ling-ling, KNEPPER J. Analysis of the imaging characteristics of the KB and KBA x-ray microscopes at non-coaxial grazing incidence[J]. *Open Physics*, 2018, **16**(1): 751-756.

[7] LI Ya-ran, MU Bao-zhong, XIE Qing, *et al*. Development of an x-ray eight-image Kirkpatrick-Baez diagnostic system for China's laser fusion facility[J]. *Applied Optics*, 2017, **56**(12): 3311-3318.

[8] VOGEL J K, PIVOVAROFF M J, KOZIOZIEMSKI B, *et al*. Design and raytrace simulations of a multilayer-coated Wolter x-ray optic for the Z machine at Sandia National Laboratories[J]. *Review of Scientific Instruments*, 2018, **89**(10): 10G113.

[9] WANG Jing-yu, CHEN Xin-gong, WANG Xiao-fang. Kirkpatrick-Baez mirror imaging simulation and comparison with Fresnel zone plate imaging[J].*Acta Photonica Sinica*, 2010, **39**(12): 2158-2162.

[10] FRIESEN H, TIEDJE H F. HEY D S, *et al*. Kirkpatrick-Baez microscope for hard X-ray imaging of fast ignition experiments[J]. *Review of Scientific Instruments*, 2013,**84**:023704.

[11] MIMURA H, TAKEI Y, KUME T, *et al*. Fabrication of a precise ellipsoidal mirror for soft X-ray nanofocusing[J]. *Review of Scientific Instruments*, 2018, **89**(9): 093104.

[12] CHEN Sheng-hao, MU Bao-zhong, MA Shuang, *et al*. Design of hard X-ray focusing telescope with a large field of view[C]. SPIE, 2014: 92721R.

[13] LI Lin, HUANG Yi-fan, WANG Yong-tian. Modern optical design[M]. 3rd ed. Beijing: Beijing Institute of Technology Press, 2018: 354.

[14] CAO Yi-qing, LU Li-jun. Aberrations of soft x-ray and vacuum ultraviolet optical systems with orthogonal arrangement of elements[J].*Journal of the Optical Society of America A*, 2017, **34**(3): 299-307.

[15] SUZUKI Y, TAKEUCHI A. Correction of spherical aberration in grazing-incidence X-ray optics by combination of spherical-concave mirrors[C].AIP Conference Proceedings, 2011, **1365**: 156-159.